

# Lifetime and Strength of Adhesive Molecular Bond Clusters between Elastic Media<sup>†</sup>

Jin Qian, Jizeng Wang, and Huajian Gao\*

Division of Engineering, Brown University, Providence, Rhode Island 02912

Received August 4, 2007. In Final Form: October 25, 2007

With a long-term objective toward a quantitative understanding of cell adhesion, we consider an idealized theoretical model of a cluster of molecular bonds between two dissimilar elastic media subjected to an applied tensile load. In this model, the distribution of interfacial traction is assumed to obey classical elastic equations whereas the rupture and rebinding of individual molecular bonds are governed by stochastic equations. Monte Carlo simulations that combine the elastic and stochastic equations are conducted to investigate the lifetime of the bond cluster as a function of the applied load. We show that the interfacial traction is generally nonuniform and for a given adhesion size the average cluster lifetime asymptotically approaches infinity as the applied load is reduced to below a critical value, defined as the strength of the cluster. The effects of elastic moduli, adhesion size, and rebinding rate on the cluster lifetime and strength are studied under strongly nonuniform distributions of interfacial traction. Although overly simplified in a number of aspects, our model seems to give predictions that are consistent with relevant experimental observations on focal adhesion dynamics.

## 1. Introduction

Most biological cells must adhere to other cells or an extracellular matrix (ECM) to perform normal physiological functions such as migration, spreading, differentiation, growth, and healing.<sup>1</sup> Adherent cells are usually exposed to mechanical stresses evoked either by the cell's own contractile machine or by a variety of external factors. Experiments have revealed that cell adhesion on a substrate is often localized to discrete contact regions called focal adhesions (FAs) that consist of multiple transmembrane ligand–receptor bonds connecting the actin cytoskeleton of the cell to the substrate.<sup>2–4</sup> Focal adhesions are micrometer-sized dense clusters of ligand–receptor bonds linked to complex assemblies of a variety of associated proteins. It is therefore interesting to study the collective behavior of a cluster of ligand–receptor bonds under stress.

A grand challenge in molecular and cellular biomechanics is to achieve the capability to effectively control cell–cell and cell–substrate interaction, for which a quantitative description of cell adhesion is a critical step. Experiments have shown that a single molecular bond has a binding energy of only  $(10–25) k_B T$ ,<sup>5</sup> which leads to a finite lifetime as a result of thermally activated bond dissociation even in the absence of an external force. This statistical nature of single molecular bonds is an important feature that must be taken into account in theories on cell adhesion. Experiments based on dynamic force spectroscopy<sup>6–8</sup> and theoretical models by Evans and Ritchie<sup>9</sup> have firmly

established the statistical theory of single molecular bonds under force. According to this theory, bond dissociation can be regarded as thermally assisted escape over a potential energy barrier.<sup>10,11</sup> The application of an external force changes the energy landscape and should therefore influence the rupture process. Indeed, both theory and experiments<sup>6–11</sup> have indicated that the average survival time of a single molecular bond decreases exponentially with increasing load level, irrespective of specific types of molecular bonds. Although such a statistical description of single molecular bonds is by now well accepted, the collective behavior of multiple molecular bonds, such as those in cell adhesion, can be much more complex and are less well understood. A single bond only has a limited lifetime whereas a cluster of bonds can survive for a much longer time because of collective effects in a stochastic ensemble.

A pioneering theoretical framework for describing the collective behavior of multiple adhesive bonds was established by Bell,<sup>12</sup> who applied the kinetic theory of chemical reactions to predict the thermodynamic competition between bond breaking and reforming. Seifert<sup>13</sup> studied the dynamic behavior of a bond cluster subjected to ramping forces. Erdmann and Schwarz<sup>14,15</sup> developed a more rigorous theory of the cluster lifetime based on the one-step master equation in stochastic dynamics.

A common assumption of the existing models of cluster adhesion is equal sharing of the applied load among all closed bonds. On the basis of this assumption, the theory of Erdmann and Schwarz<sup>14,15</sup> predicted that the cluster lifetime monotonically increases as the cluster size grows: the larger the cluster, the more stable it is. In contrast, experimental observations have shown in general that the focal adhesion size is limited to around a few micrometers.<sup>16</sup> Also, the elastic properties of the substrate were found to play an important role in the formation and growth of FAs. Stable FAs are usually found on stiff substrates, and

<sup>†</sup> Part of the Molecular and Surface Forces special issue.

\* Corresponding author. E-mail: huajian\_gao@brown.edu. Tel: +1 401 863-2626. Fax: +1 401 863-9025.

(1) Chen, X.; Gumbiner, B. M. *Curr. Opin. Cell Biol.* **2006**, *18*, 572.

(2) Zaidel-Bar, R.; Ballestrin, C.; Kam, Z.; Geiger, B. *J. Cell Sci.* **2003**, *116*, 4605.

(3) Bershadsky, A. D.; Balaban, N. Q.; Geiger, B. *Annu. Rev. Cell Dev. Biol.* **2003**, *19*, 677.

(4) Alberts, B.; Johnson, A.; Lewis, J.; Raff, M.; Roberts, K.; Walter, P. *Molecular Biology of the Cell*, 4th ed.; Garland Science: New York, 2002.

(5) Leckband, D.; Israelachvili, J. *Q. Rev. Biophys.* **2001**, *34*, 105.

(6) Florin, E. L.; Moy, V. T.; Gaub, H. E. *Science* **1994**, *264*, 415.

(7) Alon, R.; Hammer, D. A.; Springer, T. A. *Nature* **1995**, *374*, 539.

(8) Merkel, R.; Nassoy, P.; Leung, A.; Ritchie, K.; Evans, E. *Nature* **1999**, *397*, 50.

(9) Evans, E.; Ritchie, K. *Biophys. J.* **1997**, *72*, 1541.

(10) Evans, E. *Annu. Rev. Biophys. Biomol. Struct.* **2001**, *30*, 105.

(11) Evans, E. A.; Calderwood, D. A. *Science* **2007**, *316*, 1148.

(12) Bell, G. I. *Science* **1978**, *200*, 618.

(13) Seifert, U. *Phys. Rev. Lett.* **2000**, *84*, 2750.

(14) Erdmann, T.; Schwarz, U. S. *J. Chem. Phys.* **2004**, *121*, 8997.

(15) Erdmann, T.; Schwarz, U. S. *Phys. Rev. Lett.* **2004**, *92*, 1081021.

(16) Zaidel-Bar, R.; Cohen, M.; Addadi, L.; Geiger, B. *Biochem. Soc. Trans.* **2004**, *32*, 416.

cells tend to migrate toward stiffer regions when cultured on a nonhomogeneous substrate.<sup>17,18</sup> The stiffness of the cytoskeleton can change over several orders of magnitude in response to different levels of cytoskeletal stress evoked either by actin contractility or external forces.<sup>19–21</sup> It has been shown that FAs can reversibly increase or decrease in size in response to an applied force, with force per unit area (stress) maintained near a constant value at around 5.5 kPa for different types of cells.<sup>22,23</sup>

Why is there an upper size limit on focal adhesion? Can we develop models to understand the effects of the elastic properties of the substrate and cytoskeleton on the stability and strength of FAs? Motivated by these questions, in this article we build upon the previous work of Erdmann and Schwarz<sup>14,15</sup> and attempt to develop a coupled stochastic-elasticity model that aims to seamlessly unify stochastic descriptions of individual molecular bonds and elastic descriptions of interfacial traction. To avoid overcomplications of modeling at this stage, we consider an idealized theoretical model involving a cluster of molecular bonds between two semi-infinite elastic media under a tensile load. Of special interest is how the nonuniformly distributed interfacial traction influences the cluster lifetime and strength. Our approach can be extended to a broad range of situations involving nonuniform stress and/or nonhomogeneous bond density distributions. For example, when leukocytes tether to and roll on vessel walls under blood flow, the molecular bonds near the periphery of the contact region are expected to be more stretched than those at the center.<sup>24,25</sup> In cell–cell adhesion, the formation of an immunological synapse involves ligand–receptor bonds with different rest lengths, and the adhesion complex is often organized into patterns with spatially varying bond density.<sup>26</sup> The current approach could serve as a basis for the further study of such problems.

This article is organized as follows. We first derive a fundamental scaling law that controls the interfacial traction distribution based on classical elastic equations in contact mechanics. We show that, depending on the adhesion size and the relative stiffness of the surrounding elastic media with respect to the adhesion cluster, there is a transition between uniform and cracklike singular distributions of interfacial traction. Recognizing the discrete configurations of molecular bonds and the effects of random bond breaking/reforming, we then introduce the appropriate master equation describing the stochastic dynamics of cluster evolution according to spatially dependent bond rupture and rebinding rates, with each bond considered to be an independent reaction site. A Monte Carlo scheme based on the Gillespie algorithm<sup>27,28</sup> is introduced to solve the coupled stochastic-elastic equations, and a series of simulations are performed to investigate the cluster lifetime under different levels

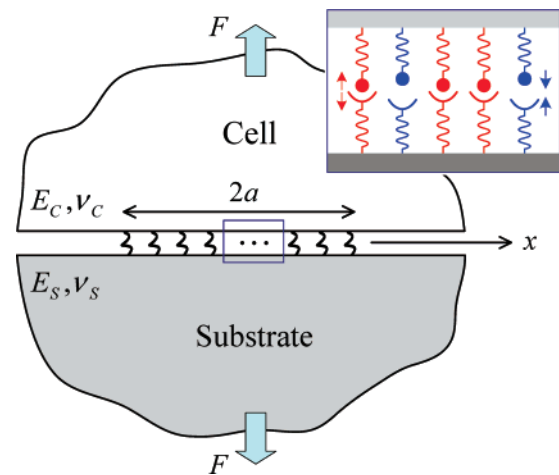


**Figure 1.** Schematic illustration of an idealized theoretical model of adhesion between two elastic bodies via a cluster of ligand–receptor bonds under a force  $F$ . The bond cluster size is  $2a$ . One side of the adhesion is an elastic medium with Young's modulus  $E_C$  and Poisson's ratio  $\nu_C$  mimicking the cell body, and the other side is a substrate with different elastic properties  $E_S$  and  $\nu_S$ .

of applied load and cluster size. For a given adhesion size, the average cluster lifetime is found to approach infinity asymptotically as the applied load is reduced to below a critical value that is then defined as the strength of the bond cluster. Our simulations show that the initial growth of a small cluster tends to stabilize adhesion as a result of collective effects in a stochastic process, in agreement with the findings of Erdmann and Schwarz.<sup>14,15</sup> However, our study also shows that as the cluster grows larger the elasticity of the system eventually results in cracklike singular stress concentration near the edge of adhesion. As a result, the cluster lifetime decreases at large cluster sizes because of cracklike propagation failure. We show that the assumption of uniform interfacial traction adopted by Erdmann and Schwarz<sup>14,15</sup> is approximately valid only for a limited range of elastic moduli and adhesion size whereas nonuniform traction distribution is a general rule. We discuss the effects of elastic moduli, adhesion size, and bond rebinding rate on the cluster lifetime and strength. Some discussions are also made comparing our simulation results to relevant experimental observations.

## 2. Model

The theoretical model under consideration is shown in Figure 1, where a cluster of ligand–receptor bonds establishes an adhesion patch of size  $2a$  between two dissimilar elastic media under an applied force of  $F$ . A number of molecular bonds are fixed within the adhesion domain at an equal spacing of  $b$ , corresponding to a bond density of  $\rho_{LR} = 1/b^2$ . In this way, only specific adhesion via ligand–receptor linkages is considered, and secondary nonspecific interactions are ignored. One side of adhesion is an elastic medium mimicking the body of a cell, and the other side represents an elastic substrate (ECM or another cell). The Young's modulus and Poisson's ratio are  $E_C, \nu_C$  for the cell and  $E_S, \nu_S$  for the substrate. In such a bimaterial contact problem, it is usually convenient to define a combined elastic modulus  $E^*$  as<sup>29</sup>

$$\frac{1}{E^*} = \frac{1 - \nu_C^2}{E_C} + \frac{1 - \nu_S^2}{E_S} \quad (1)$$

- (17) Pelham, R. J.; Wang, Y.-L. *Proc. Natl. Acad. Sci. U.S.A.* **1997**, *94*, 13661.  
 (18) Tan, J. L.; Tien, J.; Pirone, D. M.; Gray, D. S.; Bhadriraju, K.; Chen, C. *Proc. Natl. Acad. Sci. U.S.A.* **2003**, *100*, 1484.  
 (19) Discher, D. E.; Janmey, P. A.; Wang, Y.-L. *Science* **2005**, *310*, 1139.  
 (20) Gardel, M. L.; Shin, J. H.; MacKintosh, F. C.; Mahadevan, L.; Matsudaira, P.; Weitz, D. A. *Science* **2004**, *304*, 1301.  
 (21) Storm, C.; Pastore, J. J.; MacKintosh, F. C.; Lubensky, T. C.; Janmey, P. A. *Nature* **2005**, *435*, 191.  
 (22) Balaban, N. Q.; Schwarz, U. S.; Rivelino, D.; Goichberg, P.; Tzur, G.; Sabanay, I.; Mahalu, D.; Safran, S. A.; Bershadsky, A. D.; Addadi, L.; Geiger, B. *Nat. Cell Biol.* **2001**, *3*, 466.  
 (23) Rivelino, D.; Zamir, E.; Balaban, N. Q.; Schwarz, U. S.; Ishizaki, T.; Narumiya, S.; Kam, Z.; Geiger, B.; Bershadsky, A. D. *J. Cell Biol.* **2001**, *153*, 1175.  
 (24) Chang, K. C.; Tees, D. F. J.; Hammer, D. A. *Proc. Natl. Acad. Sci. U.S.A.* **2000**, *97*, 11262.  
 (25) Schwarz, U. S.; Alon, R. *Proc. Natl. Acad. Sci. U.S.A.* **2004**, *101*, 6940.  
 (26) Qi, S. Y.; Groves, J. T.; Chakraborty, A. K. *Proc. Natl. Acad. Sci. U.S.A.* **2001**, *98*, 6548.  
 (27) Gillespie, D. T. *J. Comput. Phys.* **1976**, *22*, 403.  
 (28) Gillespie, D. T. *J. Phys. Chem.* **1977**, *81*, 2340.

(29) Johnson, K. L. *Contact Mechanics*; Cambridge University Press: New York, 1985.

To account for the elasticity of the system in a simple way, we consider a slice of the system with out-of-plane thickness  $b$ .<sup>41</sup> In this formulation, one period in the out-of-plane direction is considered so that  $F$  has the usual dimension of newtons. In this setup, the total number  $N_t$  of bonds within the out-of-plane thickness of  $b$  is  $N_t = 2a/b$ . Each bond is modeled as a Hookean spring with stiffness  $k_{LR}$  until rupture.

**2.1. Continuum Modeling on Interfacial Traction: The Stress Concentration Index.** To understand how interfacial traction is distributed within the adhesion patch, let us first consider a special case when all bonds are closed. In this case, the interfacial traction can be expressed as  $\sigma(x) = \rho_{LR}k_{LR}u(x)$ , where  $x$  is a lateral coordinate along the interface with the origin located at the center of the adhesion patch and  $u(x)$  is the extension of a bond relative to its rest length under the applied force  $F$ . At any given position  $x$ , the elastic extension  $u(x)$  of the bonds and the relative normal surface displacement  $w(x)$  of the two elastic bodies should satisfy  $u(x) + w(x) = h$ , where  $h$  is a constant. Differentiating the interfacial stress  $\sigma(x)$  with respect to  $x$  while recognizing  $u'(x) = -w'(x)$  gives

$$\frac{\partial \sigma(x)}{\partial x} = -\rho_{LR}k_{LR} \frac{\partial w(x)}{\partial x} \quad (2)$$

However, the surface displacement gradient  $\partial w(x)/\partial x$  of the elastic bodies can be related to the interfacial traction  $\sigma(x)$  as<sup>29</sup>

$$\frac{\partial w(x)}{\partial x} = -\frac{2}{\pi E^*} \int_{-a}^a \frac{\sigma(s) ds}{x-s} \quad (3)$$

Combining eqs 2 and 3 yields

$$\frac{\partial \sigma(\hat{x})}{\partial \hat{x}} = \frac{2\alpha}{\pi} \int_{-1}^1 \frac{\sigma(\hat{s}) d\hat{s}}{\hat{x} - \hat{s}} \quad (4)$$

where  $\hat{x}$  and  $\hat{s}$  are coordinates normalized by the adhesion half-width  $a$  and

$$\alpha = a\rho_{LR}k_{LR} \left( \frac{1 - \nu_C^2}{E_C} + \frac{1 - \nu_S^2}{E_S} \right) \quad (5)$$

is identified as a controlling parameter to determine how interfacial traction  $\sigma(x)$  is distributed within the adhesion domain. For example, in the limit  $\alpha \rightarrow 0$ , we have the solution

$$\sigma(x) = \text{constant} \quad (6)$$

indicating that the applied force  $F$  is equally shared among all bonds within the patch, as in the assumption adopted by Erdmann and Schwarz.<sup>14,15</sup> However, in the opposite limit  $\alpha \rightarrow \infty$ , the solution becomes

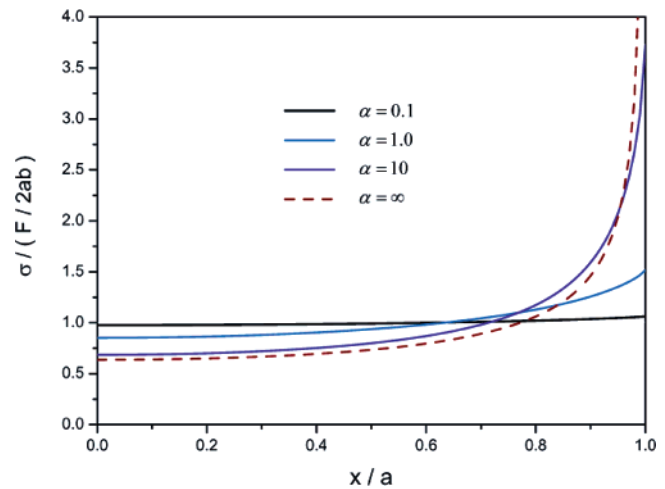


**Figure 2.** Distribution of interfacial traction for different values of the stress concentration index  $\alpha = a\rho_{LR}k_{LR}/E^*$ .

$$\sigma(x) = \frac{F}{\pi ab} \frac{1}{\sqrt{1 - x^2/a^2}} \quad (7)$$

corresponding to the interfacial traction distribution for a 2D external crack.<sup>30</sup> In this case, the stress distribution at the edge of adhesion is actually singular. For the intermediate range  $0 < \alpha < \infty$ , maximum stress generally occurs at the edge, and minimum stress appears at the center of the patch. The numerical results in Figure 2 show that, for  $\alpha$  values smaller than 0.1, the interfacial stress is nearly uniformly distributed within the adhesion patch whereas for  $\alpha$  values larger than 1 stress concentration emerges near the edge of the patch, similar to the crack singular solution in eq 7. We shall refer to  $\alpha$  as the stress concentration index.

**2.2. Elasticity Modeling of the Force Distribution on Discrete Bonds.** Before we consider the random events of dissociation/association in a group of discrete molecular bonds, we will discuss the elastic equations that will be used to determine the distribution of load on each bond. For a bond location  $x_i$  within the adhesion domain, the displacement induced by a different bond at location  $x_j$  ( $i \neq j$ ) is given by the elastic Green's function as<sup>29</sup>

$$w_{ij} = \frac{1}{\pi E^* b} 2F_j (\ln |x_\infty - x_j| - \ln |x_i - x_j|) \quad (8)$$

where  $F_j$  is the force on bond at  $x_j$  and  $x_\infty$  is an arbitrary reference point that will not influence the force calculation. To avoid singularity, the self-displacement at  $x_i$  induced by the force  $F_i$  that is modeled as an equivalent uniform pressure with half-width  $a_0$  is given by<sup>29</sup>

$$w_{ii} = -\frac{1}{\pi E^*} \frac{F_i}{2a_0 b} (2a_0 \ln 4 + C_i) \quad (9)$$

where  $a_0$  denotes the radius of individual bonds with the typical value on the order of a few nanometers<sup>31</sup> and  $C_i$  is a length constant chosen to satisfy the condition that  $F_i$  causes zero displacement at  $x_\infty$ . Applying the geometrical relation  $u(x) + w(x) = h$  at  $x_i$  where a close bond is located and substituting the linear spring law  $F_i = k_{LR}u_i$  yield

(30) Tada, H.; Paris, P. C.; Irwin, G. R. *The Stress Analysis of Cracks Handbook*, 3rd ed.; ASME Press: New York, 2000.

(31) Arnold, M.; Cavalcanti-Adam, E. A.; Glass, R.; Blümmel, J.; Eck, W.; Kantlehner, M.; Kessler, H.; Spatz, J. P. *ChemPhysChem* **2004**, *5*, 383.

(32) Chesla, S. E.; Selvaraj, P.; Zhu, C. *Biophys. J.* **1998**, *75*, 1553.

(33) Erdmann, T.; Schwarz, U. S. *Eur. Phys. J. E* **2007**, *22*, 123.

(34) Erdmann, T.; Schwarz, U. S. *Biophys. J.* **2006**, *91*, L60.

(35) van Kampen, N. G. *Stochastic Processes in Physics and Chemistry*; North-Holland: New York, 1992.

(36) Long, M.; Goldsmith, H. L.; Tees, D. F. J.; Zhu, C. *Biophys. J.* **1999**, *76*, 1112.

(37) Tees, D. F. J.; Coenen, O.; Goldsmith, H. L. *Biophys. J.* **1993**, *65*, 1318.

(38) Zuckerman, D. M.; Bruinsma, R. F. *Phys. Rev. E* **1998**, *57*, 964.

(39) Small, J. V.; Geiger, B.; Kaverina, I.; Bershadsky, A. *Nat. Rev. Mol. Cell Biol.* **2002**, *3*, 957.

(40) Wang, J.; Gao, H. *J. Mech. Phys. Solids* **2008**, *56*, 251.

(41) This is commonly referred as a plain strain problem in solid mechanics.

$$\sum_{j=1, j \neq i}^n \frac{1}{\pi E^* b} 2F_j (\ln |x_\infty - x_j| - \ln |x_i - x_j|) - \frac{1}{\pi E^* 2a_0 b} F_i (2a_0 \ln 4 + C_i) + \frac{F_i}{k_{LR}} - h = 0 \quad (10)$$

where  $n$  is the current number of closed bonds within the adhesion domain. The  $n + 1$  unknowns ( $F_1, F_2, \dots, F_n, h$ ) are solved from the above  $n$  equations together with the global force balance<sup>42</sup>

$$\sum_{i=1}^n F_i = F \quad (11)$$

Once the  $n + 1$  unknowns ( $F_1, F_2, \dots, F_n, h$ ) are obtained, the separation  $\delta_i$  between the two elastic media at  $x_i$  where an open bond is located can be calculated as

$$\delta_i = h + l_b - \left( \sum_{j=1, j \neq i}^n \frac{1}{\pi E^* b} 2F_j (\ln |x_\infty - x_j| - \ln |x_i - x_j|) - \frac{1}{\pi E^* 2a_0 b} F_i (2a_0 \ln 4 + C_i) \right) \quad (12)$$

where  $l_b$  is the rest length of the ligand–receptor bond.

### 2.3. Stochastic Modeling of Bond Dissociation/Association.

The above elasticity formulation allows us to determine the force distribution acting on each closed bond and the surface separation at each open bond within the adhesion domain at any instant during cluster evolution. However, according to single-molecule mechanics, a given bond may be closed at one instant and break at another as a result of thermally activated escape from the binding potential well.

The bond dissociation rate increases exponentially with load as<sup>12</sup>

$$k_{\text{off}} = k_0 e^{F_i/F_b} \quad (13)$$

where  $F_b$  is a force scale typically in the piconewton range and  $k_0$  is the spontaneous dissociation rate in the absence of the applied load. For bonds in focal adhesions,  $k_0$  falls in the range from a fraction of a second to around 100 s.<sup>11</sup> Chesla et al.<sup>32</sup> used a micropipette technique to measure the kinetic rate constants of individual bonds by considering the 2D diffusion of bonds between opposing surfaces.

The bond association rate,  $k_{\text{on}}$ , is assumed to depend on the separation between a ligand and receptor as described in references 33 and 34. To form a binding complex, a ligand and its complementary receptor have to come sufficiently close to each other to react. To model this process, we consider the reaction between a binding site on the substrate and a receptor tethered to the cell wall by a linear spring with stiffness  $k_{LR}$  and rest length  $l_b$ . At a given separation  $\delta$ , the probability density function for the receptor to have displacement  $u$  is<sup>33,34</sup>

$$P(u) = \frac{1}{Z} \exp\left(-\frac{k_{LR}u^2}{2k_B T}\right), u \in [-l_b, \delta - l_b] \quad (14)$$

(42) The corresponding discrete elastic equations in 3D are<sup>29</sup>

$$\frac{1}{\pi E^*} \sum_{j=1, j \neq i}^n \frac{F_j}{r_{ij}} + \frac{4}{\pi^2 E^* a_0} \frac{F_i}{r_{ij}} + \frac{F_i}{k_{LR}} - h = 0 \text{ and } \sum_{j=1}^n F_j = F$$

where  $r_{ij}$  is the distance between bond  $i$  and bond  $j$ . All the other symbols have the same definition as those in the 2D case.

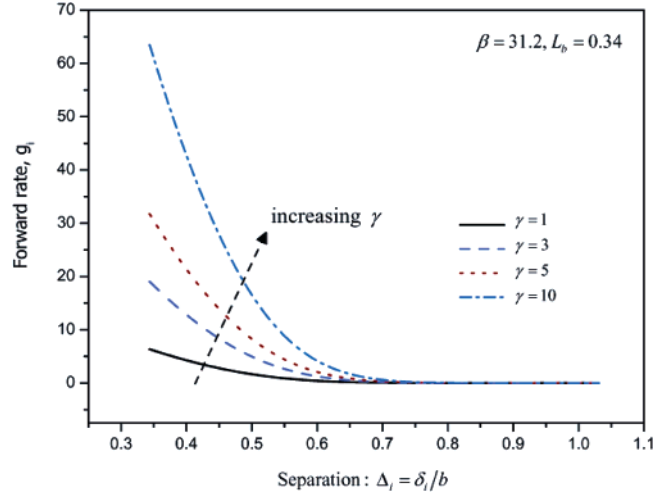


**Figure 3.** Association rate  $g_i$  of an open bond as a function of surface separation.

where the partition function  $Z$  satisfying the normalization condition  $\int_{-l_b}^{\delta-l_b} P(u) du = 1$  is

$$Z = \sqrt{\frac{\pi k_B T}{2k_{LR}}} \left( \text{erf}\left(\frac{\delta - l_b}{\sqrt{\frac{k_{LR}}{2k_B T}}}\right) + \text{erf}\left(\frac{l_b}{\sqrt{\frac{k_{LR}}{2k_B T}}}\right) \right) \quad (15)$$

The probability that the receptor comes within a reacting radius  $l_{\text{bind}}$  of the binding site is then<sup>33,34</sup>

$$p = \frac{l_{\text{bind}}}{Z} \exp\left(-\frac{k_{LR}(\delta - l_b)^2}{2k_B T}\right) \quad (16)$$

Hence, the overall association rate is

$$k_{\text{on}} = k_{\text{on}}^0 \frac{l_{\text{bind}}}{Z} \exp\left(-\frac{k_{LR}(\delta - l_b)^2}{2k_B T}\right) \quad (17)$$

where  $k_{\text{on}}^0$  is the reaction rate between the binders.

Therefore, the reverse/dissociation rate for a closed bond at location  $x_i$  can be written in a dimensionless form as

$$r_i = \frac{k_{\text{off}}}{k_0} = e^{f_i} \quad (18)$$

where  $f_i = F_i/F_b$  is the normalized bond force acting on it, and the forward/association rate for an open bond is<sup>33,34</sup>

$$g_i = \frac{k_{\text{on}}}{k_0} = 2\gamma \sqrt{\frac{\beta}{\pi}} \frac{\exp(-\beta(\Delta_i - L_b)^2)}{\text{erf}((\Delta_i - L_b)\sqrt{\beta}) + \text{erf}(L_b\sqrt{\beta})} \quad (19)$$

where  $\beta = k_{LR}b^2/(2k_B T)$ ,  $\gamma = (k_{\text{on}}^0/k_0)(l_{\text{bind}}/b)$  is a prefactor,  $\Delta_i = \delta_i/b$  is the surface separation normalized by bond spacing  $b$ , and  $L_b = l_b/b$  is the rest length of the bond after the same normalization. Note that the forward rate described above depends strongly on the surface separation. The dimensionless parameters  $\beta$  and  $L_b$  are estimated from relevant typical values listed in Table 1, which are used in the Monte Carlo simulations to be described shortly. Figure 3 plots the behavior of the forward rate  $g_i$  for different values of  $\gamma$  as the normalized surface separation  $\Delta_i$  varies between 1 and 3. Interestingly, for the range of  $\gamma$  under consideration, we see that  $g_i$  decays in a similar manner and becomes nearly zero when the opposing surfaces are separated beyond about 2 times the bond rest length. This means that the chance of rebinding is very low once the surface separation

**Table 1. List of Parameters Used in the Coupled Monte Carlo Simulations**

parameters	values
total number of bonds, $N_t$	2–100
spacing between neighboring bonds, $b$ (nm)	32
focal adhesion size, $2a$ ( $\mu\text{m}$ )	0.064–3.2
ligand–receptor bond density, $\rho_{\text{LR}}$ ( $\mu\text{m}^{-2}$ )	$\sim 1000$
single bond stiffness, $k_{\text{LR}}$ (pN/nm)	0.25
combined elastic modulus, $E^*$ (kPa)	1–1000
factor of rebinding rate, $\gamma$	1–100
rest length of bond, $l_b$ (nm)	11
force scale in bond dissociation, $F_b$ (pN)	4
radius of individual bonds, $a_0$ (nm)	5

exceeds  $2l_b$ . We expect that this strongly decaying behavior of the rebinding rate will play a very important role in our combined stochastic-elasticity theory of adhesion clusters because the surface separation is generally larger at the cluster edge than at the center and consequently rebinding is less likely to occur at the edge. Once the opposing surfaces are separated by more than a critical distance (about  $2l_b$  at our prescribed parameters), rebinding becomes impossible, and the cluster is expected to undergo cracklike failure from the adhesion edge.

We consider a cluster with all bonds closed initially. The bonds undergo stochastic breaking or rebinding described by the master equation<sup>35</sup>

$$\frac{dP_n(\tau)}{d\tau} = g_{n-1}(\tau)P_{n-1}(\tau) + r_{n+1}(\tau)P_{n+1}(\tau) - [r_n(\tau) + g_n(\tau)]P_n(\tau) \quad (20)$$

where  $\tau = k_0 t$  is the normalized time,  $P_n(\tau)$  represents the probability that  $n$  bonds are closed at time  $\tau$ , and  $r_n$  and  $g_n$  are the total dissociation and association rates for the state of  $n$  closed bonds, respectively. If the applied load  $f = F/F_b$  is equally shared among all of the  $n$  closed bonds, then we would have  $r_n = ne^{fn}$ . However, because the load  $f$  is nonuniformly distributed among closed bonds as a result of the elastic interactions, the total dissociation rate is

$$r_n = \sum_{i=1}^n e^{f_i} \quad (21)$$

It can be shown that the total dissociation rate for a uniform distribution of traction,  $r_n = ne^{fn}$ , corresponds to the minimum stationary point of  $\sum_{i=1}^n e^{f_i}$  under the condition  $\sum_{i=1}^n f_i = f$ . In other words, any spatial variation of force distribution from the uniform case would increase the total rupture probability and cause the cluster to be less stable. Therefore, assuming  $r_n = ne^{fn}$  tends to overestimate the cluster lifetime or strength.

### 3. Numerical Method

The Monte Carlo method based on Gillespie's algorithm,<sup>27,28</sup> as performed by Erdmann and Schwarz<sup>14,15</sup> under the assumption of equal load sharing by all closed bonds, can be used to solve the master equation numerically. The basic idea of such simulations is to cast stochastic trajectories for cluster evolution in accordance with the above-described reaction rates and average over many independent trials to obtain useful statistical information. At any instant during the cluster evolution, random numbers are generated to determine whether the next activity is bond breaking or rebinding and how long the next reaction will take. For our modeling with spatial degrees of freedom, it is necessary to determine where the next event should occur. Therefore, we consider each bond location to be an independent reaction site

where the next event will be bond rupture at rate  $r_i$  if the bond is currently closed and bond rebinding at rate  $g_i$  if the bond is currently open. The values of bond reaction rates,  $r_i$  and  $g_i$ , can be obtained from the force distribution among closed bonds and surface separation at open bonds calculated from the elasticity analysis. For the entire bond cluster, we have a series of reaction rates denoted as  $a_\mu$ , with  $\mu$  referring to a bond location, which is equated to the calculated  $r_i$  or  $g_i$  depending on the current bond state. Previously, a number of numerical algorithms were developed for the study of bond kinetics in cell adhesion.<sup>36,37</sup> In the present study, we apply the so-called "first reaction method"<sup>27,28</sup> of Gillespie's algorithm, following Erdmann and Schwarz.<sup>14,15</sup> We generate a series of independent random numbers  $\xi_\mu$  for individual reaction sites that are uniformly distributed over the interval  $[0, 1]$ . The time for the next reaction is chosen to be the smallest among a series of values  $d\tau_\mu$  calculated according to<sup>27,28</sup>

$$d\tau_\mu = -\frac{\ln \xi_\mu}{a_\mu} \quad (22)$$

or, in other words,

$$d\tau = \min(d\tau_\mu) \quad (23)$$

At the same time, the location for the next event is identified to be the reaction site  $\mu$  where  $d\tau$  is chosen. The event type for the next reaction is rupture if the bond at site  $\mu$  is currently closed and rebinding if it is currently open. Any change in bond state requires an update of the bond force distribution and surface separation on the elasticity part of the model, which is then used to determine the subsequent reactions. This coupling proceeds until all of the bonds within the adhesion domain are open, and the total elapsing time is recorded as the cluster lifetime. The Monte Carlo simulation based on the above algorithm is equivalent to the original master equation as long as the number of trajectories is sufficiently large. To investigate the stability of molecular bond clusters in the presence of nonuniform force distribution, we adopt the following procedure:

(1) Create an adhesion domain consisting of  $N_t$  uniformly distributed bonds. Record bond locations  $x_\mu$  (reaction sites). All bonds are set to be closed at  $\tau = 0$ .

(2) Solve the interfacial force distribution based on discrete elastic equations as formulated in eqs 10 and 11. Record forces  $f_i$  acting on each closed bond, and calculate surface separation  $\delta_i$  at each open bond according to eq 12.

(3) Calculate reaction rates  $a_\mu$  for all reaction sites:  $a_\mu = r_i$  for closed bonds, and  $a_\mu = g_i$  for open bonds.

(4) Generate a set of independent random numbers  $\xi_\mu$ , which are uniformly distributed over  $[0, 1]$ , for each individual reaction site and insert them into eq 22. Record the smallest  $d\tau_\mu$  and the corresponding  $\mu$  as the time and location associated with the next bond reaction, respectively.

(5) Change the bond state at site  $\mu$ . The bond status at site  $\mu$  is changed to open if it is currently closed and to closed if it is open. Set  $\tau = \tau + d\tau$ .

(6) Go to step 2 and loop until all bonds within the adhesion area are open. Record the final lifetime for the current trajectory.

The flow chart of this coupled numerical procedure is illustrated in Figure 4. Many such trajectories are calculated to obtain the average behavior of the bond cluster. We will discuss in the next section how the cluster lifetime is influenced by the applied load and develop a strength theory of bond clusters based on the analysis.

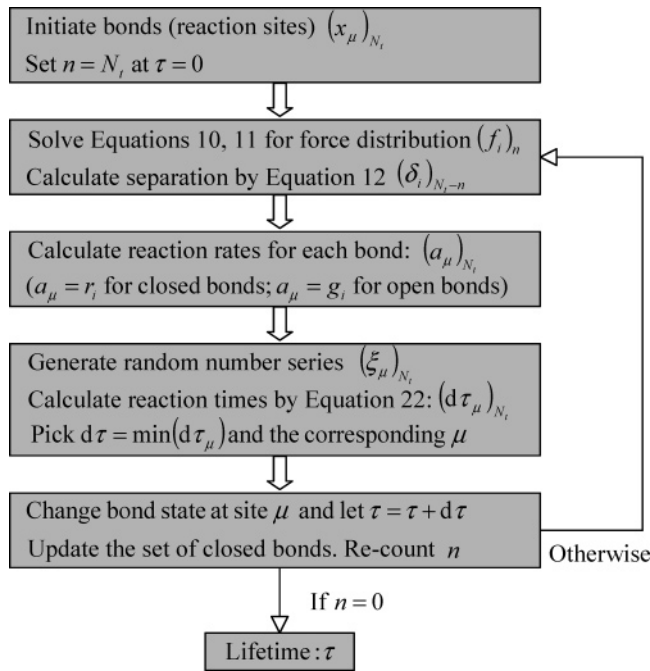


**Figure 4.** Flow chart of a Monte Carlo simulation method coupling stochastic descriptions of molecular bonds and elastic descriptions of cell–substrate interaction.

#### 4. Results and Discussions

We first simulate the lifetime of a focal adhesion cluster shown in Figure 1 that consists of 40 bonds under different levels of applied load. The spacing between neighboring bonds is set at  $b = 32$  nm, corresponding to a bond density of around  $1000 \mu\text{m}^{-2}$ . We assign  $E^* = 10$  kPa for the combined elastic modulus of the cell and substrate. The ligand–receptor bond stiffness,  $k_{LR}$ , is taken to be  $0.25$  pN/nm following an estimate for the fibronectin–integrin bond.<sup>34</sup> Under these parameters, the stress concentration index  $\alpha$  is calculated to be 16, which implies a severe stress concentration at the edge of adhesion. The force scale  $F_b$  is fixed at  $4$  pN,<sup>14,15</sup> and the radius  $a_0$  of each bond is taken as  $5$  nm.<sup>31</sup> For the rebinding rate, we set  $\gamma = 1$ <sup>33,34</sup> and  $l_b = 11$  nm.<sup>38</sup> These parameters are summarized in Table 1. We simulate the cluster lifetime by imposing different levels of load on the adhesion patch. Figure 5a plots some representative simulation trajectories for three different levels of apparent stress,  $F/2ab$ . Reducing the load generally stabilizes the cluster and leads to longer lifetime. The average lifetime ( $\tau = k_0 t$ ) over hundreds of trajectories is plotted as a function of the apparent stress  $F/2ab$  in Figure 5b. We see that the lifetime asymptotically approaches infinity as  $F/2ab$  decreases to below a critical value. Loads larger than this critical value dramatically decrease the mean lifetime and cause the cluster to be unstable. We define the cluster strength  $F_{cr}/2ab$  as the critical load at which the cluster lifetime asymptotically approaches infinity. In numerically determining the cluster strength, we pick  $\tau_\infty = 100$  (i.e., a 100-fold prolonging of  $k_0$ ). Once the mean survival time of a cluster exceeds  $\tau_\infty$ , we say that the cluster is stable under the corresponding load, and the critical load at  $\tau_\infty$  is defined as the strength. We point out that the cluster strength based on this prescribed time scale depends on the selection of  $\tau_\infty$ , but the dependence is weak because the load–lifetime curve for the cluster has a very large slope near the critical load. We find that at the load corresponding to  $\tau_\infty = 100$  a further load reduction of merely  $\sim 2\%$  would double the lifetime. Therefore, we believe that a different selection of  $\tau_\infty$ , say  $\tau_\infty = 1000$ , will lead to only a minor change in the predicted strength values.

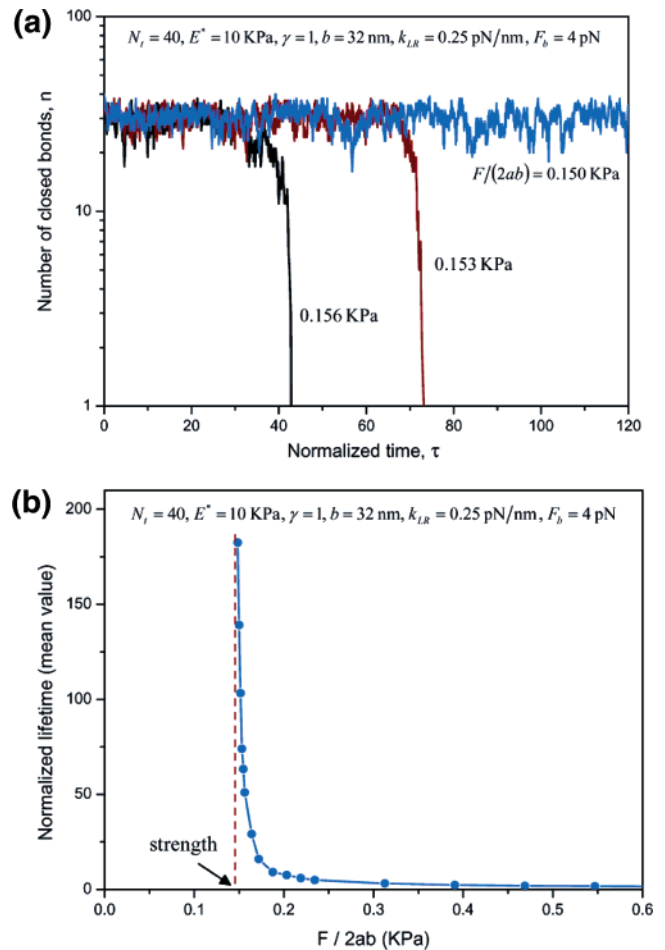


**Figure 5.** (a) Representative simulation trajectories of a molecular bond cluster of fixed size evolving under three different levels of an applied load. (b) Mean lifetime of the cluster as a function of the load. The lifetime asymptotically approaches infinity as the load reaches a critical value defined as the cluster strength.

To investigate the size effects on cluster strength, we have performed a series of Monte Carlo simulations by varying the number of bonds from 2 to 100. For the chosen bond spacing of  $b = 32$  nm, the adhesion domains under investigation have sizes ranging from  $64$  nm to  $3.2 \mu\text{m}$ . We consider different values of the combined elastic modulus  $E^*$  between  $1$  kPa and  $1$  MPa. The rebinding rate factor  $\gamma$  is set to be  $1.0$ . In the results drawn in Figure 6a, we observe that clusters with fewer than four bonds possess a limited lifetime even in the absence of the applied load, similar to the behavior of a single bond. Their strengths are considered to be zero. Clusters with more than four bonds begin to exhibit long-term stability under a finite load because of the collective effect of clustering. At a fixed cluster size, increasing the combined elastic modulus generally results in a stronger, more stable cluster. This can be understood from the point of view that a high elastic modulus decreases the stress concentration index  $\alpha$  toward the regime of uniform interfacial traction. At  $E^* = 1$  MPa, the cluster strength monotonically increases with the growing cluster size within the calculated adhesion size, which is similar to the results based on the equal-load-sharing assumption considered by Erdmann and Schwarz<sup>14,15</sup> that essentially corresponds to a cluster of bonds between two rigid bodies ( $E^* = \infty$ ). The stress concentration index  $\alpha$  is 4 for  $N_i = 100$  and  $E^* = 100$  kPa, suggesting a moderate stress concentration near the patch edge. Our simulation results suggest that this extent of nonuniform force distribution has induced cracklike failure of the cluster, as reflected by the fact that the cluster strength

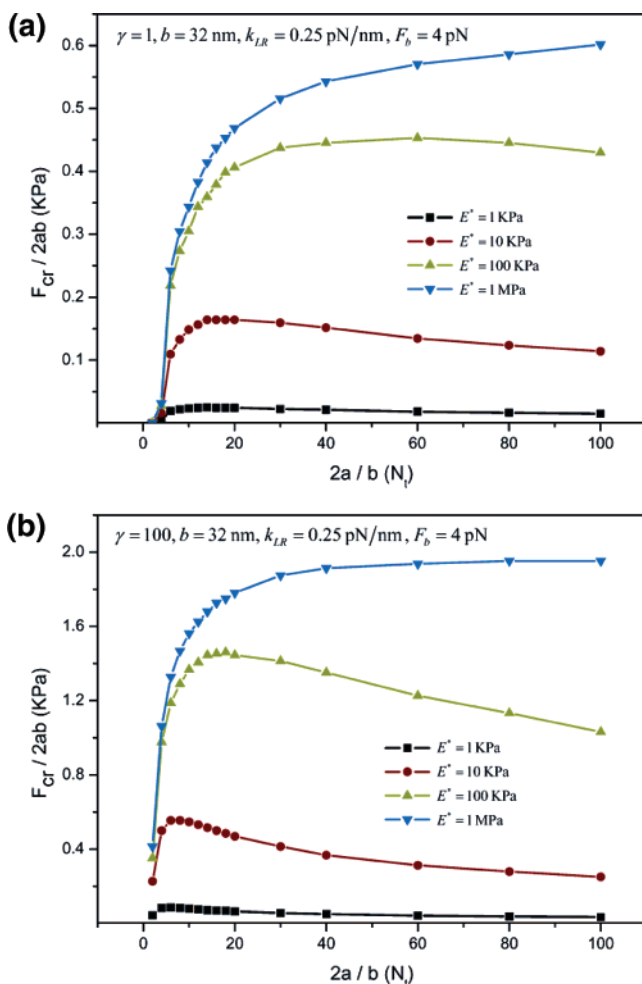


**Figure 6.** Strength of a molecular bond cluster as a function of adhesion size for different values of the combined elastic modulus  $E^*$  from 1 kPa to 1 MPa. The rebinding-rate factor,  $\gamma$ , is taken as (a)  $\gamma = 1$  and (b)  $\gamma = 100$ .

decreases with increasing cluster size. The effects of stress concentration are more pronounced for lower values of the elastic moduli, as indicated by the curves for  $E^* = 10$  kPa and  $E^* = 1$  kPa in Figure 6a.

We notice that the calculated strength values are quite low under the present parameters (e.g.,  $\sim 0.4$  kPa for  $N_t = 100$ ,  $E^* = 100$  kPa, and  $\gamma = 1$ , corresponding to a load level of 0.4 pN/bond). In recognizing its exponential dependence on the applied force, we expect that the dissociation rate will be significantly enhanced by the elevated stress at the adhesion edge. This effect will be more pronounced at higher load levels at which the cluster strength should also become more sensitive to the elastic modulus and adhesion size.

A higher rebinding rate causes the cluster to become stronger and the cluster strength to be more sensitive to the elastic modulus and adhesion size. To confirm this, we consider a different type of bond with higher affinity,  $\gamma = 100$ . All of the other parameters remain the same as in the case of  $\gamma = 1$ . Figure 6b plots the cluster strength as a function of the adhesion size when the combined elastic modulus is chosen to be between 1 kPa and 1 MPa. This rebinding rate provides a stronger stabilizing effect on the bond cluster, and as a result, clusters with as few as two bonds can achieve a long lifetime at a finite force. In this case, the bond strength is indeed more sensitive to the combined elastic modulus of the system and to the adhesion size. At a fixed cluster size, increasing  $E^*$  tends to stabilize and strengthen the cluster by removing the stress concentration. The cluster strength also

shows strong size effects. For the curve corresponding to  $E^* = 100$  kPa in Figure 6b, there is an optimal size of around 20 bonds that gives rise to a maximum cluster strength. Clusters larger than this size are less stable because cracklike failure occurs as a result of the high stress concentration near the adhesion edge. The curves for  $E^* = 10$  and 1 kPa show similar behaviors with maximum strength at an optimal adhesion size. For the curve of  $E^* = 1$  MPa in Figure 6b, including that in Figure 6a, our simulations did not capture the optimal size because we have limited our simulations to clusters with fewer than 100 bonds. We believe that sufficiently large clusters will eventually encounter a severe stress concentration and will present catastrophic cracklike failure from the adhesion edge. The concept of optimal adhesion size for the maximum strength should be a general feature of molecular adhesion clusters because of statistical effects on small scales and cracklike failure on large scales. The effects of adhesion size and elastic modulus on the cluster strength can be explained on the basis of the stress concentration index  $\alpha$ : increasing adhesion size or decreasing elastic modulus tends to increase  $\alpha$  toward the regime of cracklike stress concentration, hence comprising the stability and strength of the cluster.

The maximum cluster strength at an optimal adhesion size serves as a critical threshold for adhesion. Stress levels higher than this value destabilize the clusters to the regime of limited lifetime for clusters of any size. For a nonzero applied load below the threshold, there exists a size window for stable adhesion. Clusters within this size window have strengths that are higher than the applied load, and clusters outside the window have strengths that are lower than the load. On the basis of the definition of cluster strength, clusters within the size window will achieve long-term stability, and clusters outside the window have limited lifetimes. It is therefore interesting to plot the cluster lifetime as a function of adhesion size at a fixed load level, as shown in Figure 7. We replotted in Figure 7a the curve of  $E^* = 10$  kPa in Figure 6b for a closer examination of the size effect on cluster strength. In this calculation, we take an apparent stress of 0.53 kPa. Figure 7b plots some representative simulation trajectories for three cluster sizes under this fixed load. We see that a prolonged lifetime is possible only for clusters with around 10 bonds (within an out-of-plane thickness equal to the bond spacing). Smaller clusters are not stable because the number of bonds is insufficient to achieve long-term stability and the behavior of the cluster is similar to that of a single bond. However, larger clusters also have a limited lifetime because of the elasticity induced stress concentration that tends to focus the action on a small number of bonds near the edge of the adhesion patch. The normalized mean lifetime of molecular bond clusters is plotted in Figure 7c as a function of adhesion size. The results clearly display a size window beyond which clusters cannot achieve long-term lifetime under the load. The corresponding results based on the assumption of equal load sharing would show a monotonously increasing cluster lifetime with growing cluster size. In contrast, our results show that a prolonged lifetime is possible only for clusters of intermediate size when the elasticity of the system is considered. Small adhesion size leads to single-molecule-like behavior because of statistical effects whereas large adhesion also leads to single-molecule-like behavior because of the focusing effect of the stress concentration that confines the bond rupture/dissociation events to a smaller number of bonds near the adhesion edge.

Although we do not expect that the highly idealized stochastic-elasticity model considered in this article can capture the complexity of real focal adhesion, it seems that our analysis still

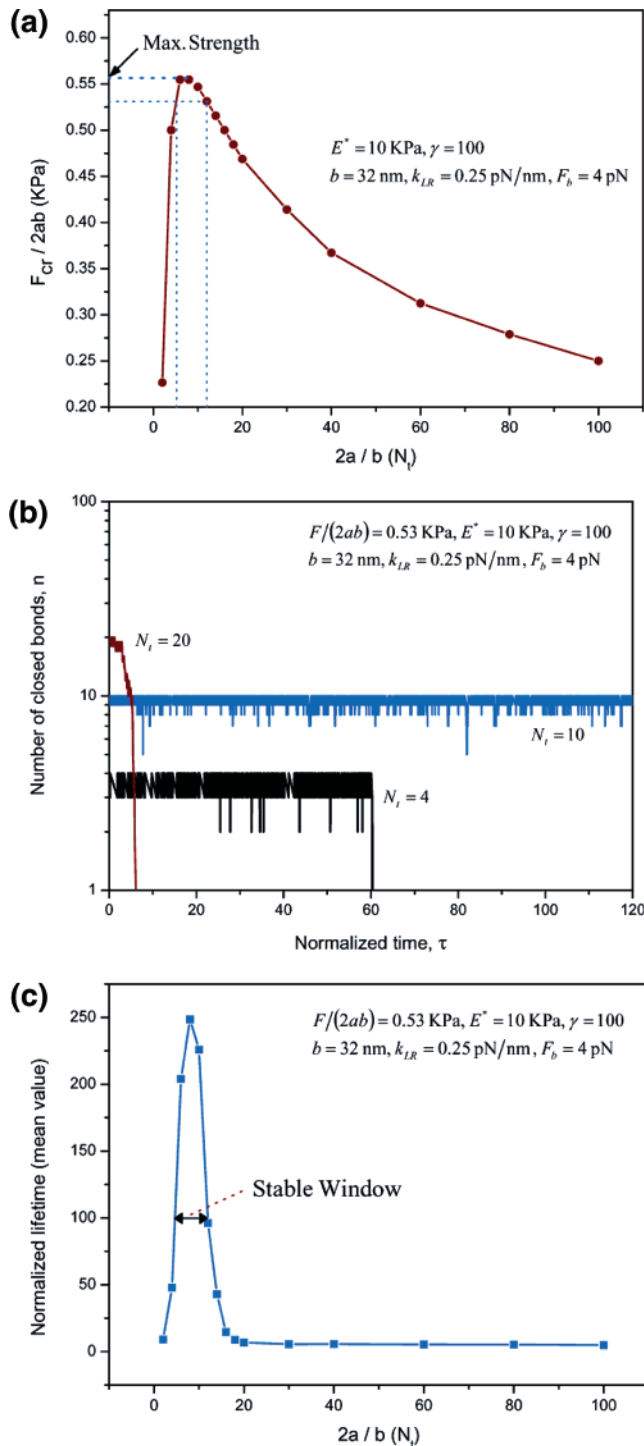


**Figure 7.** (a) Strength of a molecular bond cluster as a function of adhesion size for  $E^* = 10$  KP and  $\gamma = 100$ . (b) Representative simulation trajectories for three different cluster sizes under a fixed load of 0.53 kPa. (c) Mean cluster lifetime as a function of adhesion size at the fixed load. The results show a size window beyond which clusters cannot achieve long-term stability.

provides some feasible explanations for a range of experimental observations. First, our model shows that increasing the combined elastic modulus of the cell–substrate system helps to stabilize multiple adhesive bonds by removing the stress concentration in the adhesion domain. This is at least in qualitative agreement with the observations that stable, large FAs are formed only on sufficiently rigid substrates. The definition of the combined elastic modulus in eq 1 implies that very soft substrates will dominate over the property of the cell in that cracklike interfacial traction

will persist irrespective of the cytoskeleton stiffness, which may prevent short-lived focal complexes from maturing into large FAs. On hard substrates, the combined elastic modulus tends to be dominated by the stiffness of the cytoskeleton. This would allow the cell to control adhesion/de-adhesion actively by monitoring the contractile forces in stress fibers connecting to an FA. Generally speaking, a larger number of bonds and more uniform interfacial traction tend to stabilize molecular adhesion. From this point of view, rigid substrates, cytoskeleton stiffening via contractile forces, and intermediate adhesion size are some of the factors that contribute to stable cell adhesion whereas soft substrates, cytoskeleton softening by dissolution of the actin network, and extreme adhesion size are factors that tend to destabilize cell adhesion.

Our model provides a simple answer to the question of why FAs usually fall into a narrow size range from a few hundred nanometers to a few micrometers. Small adhesions are unstable because of the statistical nature of molecular bonds. There exists a critical cluster size for transition from single-molecule-like behavior to stable adhesion patch behavior. However, the growth of an adhesion patch ultimately leads to cracklike singular interfacial traction, hence becoming self-limiting. Therefore, the upper size limit on FAs can be understood from the point of view of severe stress concentration induced by the elastic interactions between the cell and substrate via molecular bonds. These results are all qualitatively consistent with relevant experimental observations.

## 5. Conclusions

We have developed an idealized stochastic-elasticity model of two elastic bodies joining over an adhesion patch consisting of multiple molecular bonds. The model is aimed at the seamless unification of elastic descriptions of adhesive contact on large scales and statistical descriptions of single-bond behaviors on small scales. A series of Monte Carlo simulations have been conducted to investigate how the lifetime and strength of a molecular cluster are influenced by the adhesion size, the bond rebinding rate, and the elastic stiffness of the cell–substrate system. The main conclusions of the present work are summarized as follows.

(1) Coupled stochastic-elasticity equations have been used to model the stability and strength of a patch of molecular bonds joining two elastic bodies with spatially nonuniform interfacial traction for different elastic moduli and adhesion sizes. In principle, the approach may be extended to other related problems such as leukocyte rolling and immunological synapse formation. A Monte Carlo-based numerical procedure has been employed to solve the coupled stochastic-elasticity governing equations numerically.

(2) A dimensionless parameter,  $\alpha = a\rho_{LR}k_{LR}((1 - \nu_C^2)/E_C + (1 - \nu_S^2)/E_S)$ , has been identified as a controlling factor in determining how the interfacial traction is distributed within the adhesion domain. When  $\alpha$  is small, the applied load is equally shared among closed bonds, and the cluster behavior is similar to that studied by Erdmann and Schwarz.<sup>14,15</sup> However, when  $\alpha$  is large, severe stress concentration and cracklike failure occur at the adhesion edge.

(3) Our analysis shows that the combined elastic modulus of the cell and substrate plays an important role in controlling the interfacial force distribution and cluster stability. On very soft substrates, cracklike interfacial traction cannot be alleviated by cytoskeleton stiffening,<sup>19–21</sup> which may prevent short-lived focal complexes from maturing into large FAs. On relatively stiff substrates, cells can actively control the cytoskeleton stiffness

via their motor contractile machinery. In this case, cytoskeleton stiffening can alleviate the stress concentration and allow the focal adhesions to achieve long-term stability. This is consistent with experimental observations that focal adhesions formed on stiff substrate are generally more stable than those on softer substrates.

(4) Adhesion size also plays an important role in controlling the bond force distribution and cluster stability. Growing adhesion size ultimately leads to highly nonuniform interfacial traction, which tends to destabilize cluster adhesion via cracklike failure. Our analysis shows that the cluster lifetime is prolonged only within an optimal size window. The lower bound of the window is associated with the transition from single-molecule-like behavior with a finite lifetime to statistically stable adhesion, whereas the upper bound is due to cracklike failure at large sizes.

Finally, we point out some critical assumptions made in our model in mimicking focal contacts in cell adhesion. The present study on FA dynamics has been conducted under an idealized framework based on elasticity theory and stochastic binding/unbinding whereas experiments are often focused on the biological

roles of specific proteins in cell adhesion.<sup>39</sup> We have assumed immobile ligand–receptor bonds at the cell–substrate interface. In reality, bond diffusion is likely to be important and should be incorporated into future research.<sup>40</sup> We have limited ourselves to elastic systems in the sense that any bond association–dissociation event is sensed instantly by the cell and substrate whereas real biological cells could show much more complex nonlinear and viscoelastic constitutive behaviors. We have considered only a normal load with all bonds stretched in the same direction and, in doing so, have ignored the effects of tangential forces. In contrast, the loading conditions at focal adhesion sites can be much more complex with a significant amount of tangential force. In spite of these limitations, it is encouraging that the predicted behaviors of such an idealized model are essentially consistent with relevant experimental observations. The development of more sophisticated models/approaches is currently underway.

LA702401B